

## **Computing Displacements in Transversely Isotropic Rocks Using Influence Charts**

By

**C. D. Wang and J. J. Liao**

Department of Civil Engineering, National Chiao-Tung University, Hsinchu, Taiwan,  
Republic of China

### **Summary**

This paper presents a simple graphical method for computing the displacement beneath/at the surface of a transversely isotropic half-space subjected to surface loads. The surface load can be distributed on an irregularly-shaped area. The planes of transverse isotropy are assumed to be parallel to the horizontal surface of the half-space. Based on the point load solutions presented by the authors, four influence charts are constructed for calculating the three displacements at any point in the interior of the half-space. Then, by setting  $z = 0$  of the derived solutions, another four influence charts for computing the surface displacements can also be proposed. These charts are composed of unit blocks. Each unit block is bounded by two adjacent radii and arcs, and contributes the same level of influence to the displacement. Following, a theoretical study was performed and the results showed that the charts for interior displacements are only suitable for transversely isotropic rocks with real roots of the characteristic equation; however, the charts for surface displacements are suitable for all transversely isotropic rocks. Finally, to demonstrate the use of the new graphical method, an illustrative example of a layered rock subjected to a uniform, normal circular-shaped load is given. The results from the new graphical method agree with those of analytical solutions as well. The new influence charts can be a practical alternative to the existing analytical or numerical solutions, and provide results with reasonable accuracy.

### **1. Introduction**

In the design of foundations on rocks, the deformation response of the materials is an important factor. Conventionally, foundation materials are assumed to be linearly elastic and isotropic for calculating the stresses, strains and displacements. However, for most rocks, such as foliated metamorphic, stratified sedimentary, and regularly jointed rocks, their responses to deformation exhibit some degree of anisotropy. Hence, isotropic elasticity is not suitable for computing the stresses, strains, and displacements in these rocks.

To calculate the stress, strain, and displacement in an anisotropic half-space, one can use the closed-form solutions, numerical methods, or graphical methods.

Most of the existing closed-form solutions are limited to solving plane strain or axisymmetric problems with simple boundary conditions, such as loading types and shapes. The detailed review of the exact solutions for anisotropic media can be referred to Wang and Liao (1998a). In the past few decades numerical techniques have been developed for calculating the stresses, strains, and displacements underneath an irregular-shaped foundation (Wang and Liao, 1998b). Through the use of computer, these numerical methods can easily be automated and hence can be efficient to use. However, most of them contributed to the calculation of stresses or displacements in isotropic media.

Several graphical methods for computing the displacements in an isotropic half-space have been used for decades. A graphical method using influence charts was first proposed by Newmark (1947). The influence charts are efficient to use in calculating displacement as compared to other complex mathematical or numerical methods. However, the advantages of Newmark charts diminish if the loading area is not uniform, or displacements at multiple depths are sought simultaneously. Uzan et al. (1980) constructed influence charts for a special case of a two-layer system underlain by a rigid base. Nevertheless, the charts proposed by Uzan et al. (1980) were prepared for the materials with special elastic constants; hence, the applications are restricted. Recently, Huang (1995) extended the Newmark method to construct diagrams for computing the displacement in an isotropic solid subjected to an embedded distributed uniform vertical load. Poulos (1967) proposed a graphical method, called the sector method, for calculating the displacements in an elastic half-space. All of the existing graphical methods are limited to isotropic media. To the authors' knowledge, no graphical method of displacement calculation has been proposed for anisotropic media. The aim of this paper is to construct the new influence charts for calculating the displacements in a transversely isotropic half-space subjected to three-dimensional loads with an irregular shape. By superposition of values corresponding to the influence charts, the three displacements at any point in the half-space can be estimated. This paper describes the background of the new influence charts and their application procedure. An illustrative example is presented at the end of the paper to demonstrate the procedure of computing induced interior and surface displacements using the proposed influence charts in a layered rock mass. Verifications are also made by comparing the graphical solutions (by the influence charts) with the analytical solutions.

## **2. Deformability Anisotropy of Transversely Isotropic Rocks**

Anisotropy is a general characteristic of foliated metamorphic rocks (e.g., argillite, slate, schist, phyllite, gneiss), stratified sedimentary rocks (e.g., shale, sandstone, coal, limestone), and regularly jointed rock masses. Deformability anisotropy implies that the deformability of a material is direction dependent. Depending on the planes of elastic symmetry, rock can be of general anisotropy, orthotropy, transverse isotropy, or complete isotropy. For a transverse isotropic rock, there is an axis of symmetry of rotation. The rock has isotropic properties in planes

normal to this axis. The deformability of a transversely isotropic material can be expressed in terms of five elastic constants, i.e.,  $C_{11}$ ,  $C_{13}$ ,  $C_{33}$ ,  $C_{44}$ ,  $C_{66}$  (Wang and Liao, 1998b). These constants are directly related to the engineering elastic constants  $E$ ,  $E'$ ,  $\nu$ ,  $\nu'$ , and  $G'$  as:

$$C_{11} = \frac{E \left( 1 - \frac{E}{E'} \nu'^2 \right)}{(1 + \nu) \left( 1 - \nu - \frac{2E}{E'} \nu'^2 \right)}, \quad C_{13} = \frac{E \nu'}{1 - \nu - \frac{2E}{E'} \nu'^2}, \quad (1)$$

$$C_{33} = \frac{E'(1 - \nu)}{1 - \nu - \frac{2E}{E'} \nu'^2}, \quad C_{44} = G', \quad C_{66} = \frac{E}{2(1 + \nu)}.$$

Where  $E$ ,  $E'$  are the Young's moduli in the plane of transverse isotropy and its normal, respectively;  $\nu$ ,  $\nu'$  are the Poisson's ratios characterizing the lateral strain in the plane of transverse isotropy to a normal stress acting parallel and normal to it, respectively; and  $G'$  is the shear modulus in planes normal to the plane of transverse isotropy. These engineering elastic constants can be determined by static or dynamic experiments in the laboratory. Readers can refer to Wang and Liao (1998b) for details of these methods.

### 3. Construction of the Displacement Influence Charts for a Loaded Transversely Isotropic Half-Space

Similar to the Newmark charts (1947) for isotropic materials, the proposed charts for transversely isotropic media contain systematic unit blocks. Two radial lines and two adjacent arcs bound each block. The radii of the circles relate to the depth of the interested point for interior displacements, or the base length of loading area for surface displacements in the half-space. The influence value of any unit block in displacement should be equal and independent of its location in the chart. To facilitate block counting, the plan of the surface load is drawn to a scale related to the depth of the interested point (for interior displacements) or the base length (for surface displacements). The unit blocks are made roughly square. The number of the blocks covered by the scaled loaded area is then counted.

Combining the solutions for displacements induced by different sectors with uniform loads (one of the sectors as shown in Fig. 1), one can obtain the displacements at point C with depth  $u_i z$  due to the uniform load on a unit block. Selecting proper values of coefficients in the closed-form solutions for the displacements at point C, one can obtain the values of the radii and the central angle, which form the unit block, for the influence displacements being a uniform amount, i.e. 0.004 or 0.01. In this section, the solutions for the displacements at a depth  $u_i z$  under the vertex of a uniformly loaded sector of a circle in a transversely isotropic half-space are presented first. Then, four independent influence charts for calculating the three interior displacements are proposed. Furthermore, by setting  $z = 0$  (at the surface) of the derived solutions, another four charts for calculating the surface displacements can also be proposed.

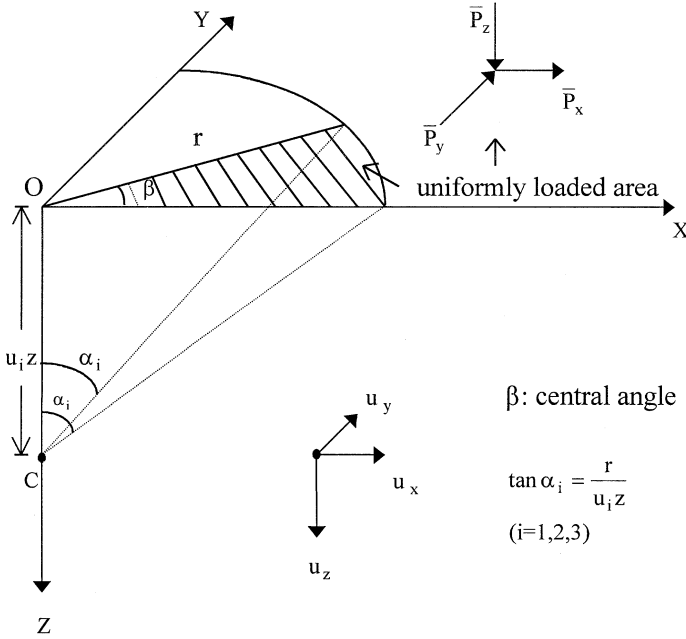


Fig. 1. Uniformly loaded sector area

### 3.1 Interior Displacements under the Vertex of a Uniformly Loaded Sector

The solutions of displacements in a transversely isotropic half-space subjected to a point load have been derived by several investigators (e.g., Liao and Wang, 1998). By integrating the point load solutions, one can obtain the displacements in the half-space, subjected to a uniform surface load of any irregularly-shaped area. Details of deriving displacements under the vertex of a uniformly loaded sector of a circle in a transversely isotropic half-space, based on the point load solutions of Liao and Wang (1998), are described as follows:

Figure 1 shows that a uniform load,  $\bar{P}_j$  ( $j = x, y, z$ , forces per unit of area) acts on a sector bounded by two radial lines and a circle arc. In the figure, the depth of point  $C(0, 0, u_{i,z})$  under the vertex is  $u_{i,z}$ , the radius is  $r$ , and the central angle is  $\beta$  (positive counterclockwise with respect to X co-ordinate axis). Consider an elementary area of  $rdrd\beta$  in the sector, the displacement at point C,  $[U]^C$ , is derived by integrating the point load solutions (Liao and Wang, 1998) with  $dr$  from 0 to  $r$  and  $d\beta$  from 0 to  $\beta$  (Gradshteynn and Ryzhik, 1994) as:

$$[U]^C = \int_0^\beta \int_0^r [U]^p r dr d\beta, \quad (2)$$

where  $[U] = [u_x, u_y, u_z]^T$  (superscript  $T$  denotes the transpose of matrix); the superscript  $C$  denotes the point C at which the induced displacements are evaluated; the superscript  $p$  indicates a point load acting at point O. Upon integration,

$[U]^C$  has the following components:

$$\begin{aligned}
 u_x^C = & \bar{P}_x z \left( -ku_1 * c\mathbf{F}_1 + \frac{kmu_2}{u_1} * c\mathbf{F}_2 + \frac{1}{C_{44}} * c\mathbf{F}_3 \right. \\
 & \left. + ku_1 * e\mathbf{G}_1 - \frac{kmu_2}{u_1} * e\mathbf{G}_2 + \frac{1}{C_{44}} * e\mathbf{G}_3 \right) \\
 & + \bar{P}_y z \left( ku_1 * d\mathbf{G}_1 - \frac{kmu_2}{u_1} * d\mathbf{G}_2 + \frac{1}{C_{44}} * d\mathbf{G}_3 \right) \\
 & + \bar{P}_z ku_2 z (u_1 * a\mathbf{H}_1 - m * a\mathbf{H}_2), \tag{3}
 \end{aligned}$$

$$\begin{aligned}
 u_y^C = & \bar{P}_x z \left( ku_1 * d\mathbf{G}_1 - \frac{kmu_2}{u_1} * d\mathbf{G}_2 + \frac{1}{C_{44}} * d\mathbf{G}_3 \right) \\
 & + \bar{P}_y z \left( -ku_1 * c\mathbf{F}_1 + \frac{kmu_2}{u_1} * c\mathbf{F}_2 + \frac{1}{C_{44}} * c\mathbf{F}_3 \right. \\
 & \left. - ku_1 * e\mathbf{G}_1 + \frac{kmu_2}{u_1} * e\mathbf{G}_2 - \frac{1}{C_{44}} * e\mathbf{G}_3 \right) \\
 & + \bar{P}_z ku_2 z (u_1 * b\mathbf{H}_1 - m * b\mathbf{H}_2), \tag{4}
 \end{aligned}$$

$$\begin{aligned}
 u_z^C = & \bar{P}_x kz (mu_1 * a\mathbf{H}_1 - u_2^* * a\mathbf{H}_2) + \bar{P}_y kz (mu_1 * b\mathbf{H}_1 - u_2^* * b\mathbf{H}_2) \\
 & + 2\bar{P}_z ku_1 u_2 z (m * c\mathbf{F}_1 - u_2 * c\mathbf{F}_2). \tag{5}
 \end{aligned}$$

where:

- $m = \frac{(C_{13}+C_{44})u_1}{C_{33}u_1^2-C_{44}}$ ,  $k = \frac{(u_1+u_2)C_{11}}{u_1u_2^2(m-u_1)(C_{11}C_{33}-C_{13}^2)}$ ;  $a = \sin \beta$ ,  $b = 1 - \cos \beta$ ,  $c = \frac{\beta}{2\pi}$ ,  $d = \frac{1-\cos 2\beta}{2}$ ,  $e = \frac{\sin 2\beta}{2}$ ;  $\mathbf{F}_i = \frac{1}{2} \left( \frac{1}{\cos \alpha_i} - 1 \right)$ ,  $\mathbf{G}_i = \frac{1}{4\pi} \left( -1 + \frac{1}{\cos \alpha_i} - 2 \ln \left| \frac{1+\cos \alpha_i}{2 \cos \alpha_i} \right| \right)$ ,  $\mathbf{H}_i = \frac{1}{2\pi} \left( \tan \alpha_i - \ln \left| \frac{1+\sin \alpha_i}{\cos \alpha_i} \right| \right)$ , and  $\tan \alpha_i = r/u_i z (i = 1, 2, 3)$ ;
- $u_3 = \sqrt{C_{66}/C_{44}}$ ;  $u_1$  and  $u_2$  are the roots of the following characteristic equation:

$$u^4 - su^2 + q = 0, \tag{6}$$

where  $s = \frac{C_{11}C_{33}-C_{13}(C_{13}+2C_{44})}{C_{33}C_{44}}$ ,  $q = \frac{C_{11}}{C_{33}}$ . If the strain energy is assumed to be positive definite in the medium (Amadei et al., 1987), the roots of Eq. (6),  $u_1$  and  $u_2$  are restricted to the following three cases:

- case 1.* When  $s^2 - 4q > 0$ ,  $u_{1,2} = \pm \sqrt{\frac{1}{2} [s \pm \sqrt{(s^2 - 4q)}]}$  are two real distinct roots;
- case 2.* When  $s^2 - 4q = 0$ ,  $u_{1,2} = \pm \sqrt{s/2}$ ,  $\pm \sqrt{s/2}$  are real double roots (i.e., complete isotropy);
- case 3.* When  $s^2 - 4q < 0$ ,  $u_1 = \frac{1}{2} \sqrt{(s + 2\sqrt{q})} - i \frac{1}{2} \sqrt{(-s + 2\sqrt{q})} = \gamma - i\delta$ ,  $u_2 = \gamma + i\delta$  are two conjugate complex roots [where  $\gamma$  cannot be equal to zero (Liao and Wang, 1998)].

Using engineering elastic constants, the following criterion can distinguish the

root type of Eq. (6).

$$\left(\frac{G}{G'}\right)^2 (1 + \nu) - \left(\frac{E}{E'}\right) \left[ 1 - \nu + \left(\frac{E}{G'}\right) \nu' - 2 \left(\frac{E}{E'}\right) \nu'^2 \right] \begin{array}{l} > 0, \text{ for case 1} \\ = 0, \text{ for case 2.} \\ < 0, \text{ for case 3} \end{array} \quad (7)$$

Gerrard (1975) and Amadei et al. (1987) demonstrated that, for most transversely isotropic rocks, the values of  $E/E'$  and  $G/G'$  are between 1 and 3, the Poisson's ratios  $\nu$  and  $\nu'$  are between 0.15 and 0.35, and the value of  $\nu'E/E'$  is between 0.1 and 0.7. Based on these data, Liao and Wang (1998) presented that approximately two thirds of transversely isotropic rocks belong to the case 1 (i.e., two real distinct roots).

### 3.2 Influence Charts for the Interior Displacements

Presented displacement influence charts include an index length representing the depth of the desired point, and numbers of concentric circles and radial lines. A unit block, except for those adjacent to the point C, is formed by two radial lines and two concentric circle arcs.  $[U]^C$  depends on the geometry of the loaded sector as described in Eqs. (3)–(5). The geometry is defined by a set of coefficients  $a, b, c, d, e, F_i, G_i$  and  $H_i$ . The values of  $a, b, c, d$  and  $e$  depend on the central angle  $\beta$ . The coefficients  $F_i, G_i$  and  $H_i$  relate to the ratio of  $r/u_i z$ . The value of  $c$  is positive regardless of the value of  $\beta$ . The others (i.e.,  $a, b, d$  and  $e$ ) can be either positive or negative. For a given depth  $u_i z$ , the values of  $F_i, G_i, H_i$  only depend on the radius  $r$ , and  $F_1 = F_2 = F_3, G_1 = G_2 = G_3, H_1 = H_2$ . Hence, only the charts for  $aH_i, bH_i, cF_i, dG_i$ , and  $eG_i$  are required for estimating  $[U]^C$  in a half-space graphically. The data of  $r$  are calculated using the Newton-Raphson method. Combining the numerical value to be 0.4% of a unit load intensity, a series of  $\beta$  and  $r$  can be obtained for  $aH_i, bH_i, dG_i$ , and  $eG_i$ , and 1% of a unit load intensity for  $cF_i$ , respectively. Considering the symmetric properties of triangular functions, the charts for  $aH_i$  and  $bH_i$  are identical, except that the X- and Y-axes are exchanged. Consequently, only four independent charts (i.e.,  $aH_i, cF_i, dG_i, eG_i$ ) are needed for computing  $[U]^C$ . Figures 2–5 depict the influence charts of  $aH_i, cF_i, dG_i$  and  $eG_i$ , respectively. The index length of depth  $u_i z$  in these figures is set to 0.8 cm. The calculated  $r$  is symmetrical with respect to the original point O, therefore, only one quarter of the chart is drawn. The sign “–” in the figures indicates that the values of  $a, b, d$  and  $e$  are negative. The influence value is negative for the blocks with a “–” sign. The details of the preparation of the influence charts can be referred to Wang and Liao (1998b).

For the medium with conjugate complex roots of the characteristic equation [Eq. (6)], the value of  $u_i z$  is a complex variable. Hence, the presented four influence charts are not suitable for computing the displacements in a transversely isotropic half-space categorized into case 3. For case 3 material, the preparation of influence charts requires elastic constants as a prior and  $u_i z$  being replaced by  $z$ . This means that the charts prepared for case 3 material are valid only for a particular medium. The Appendix illustrates the method for constructing the influence chart and

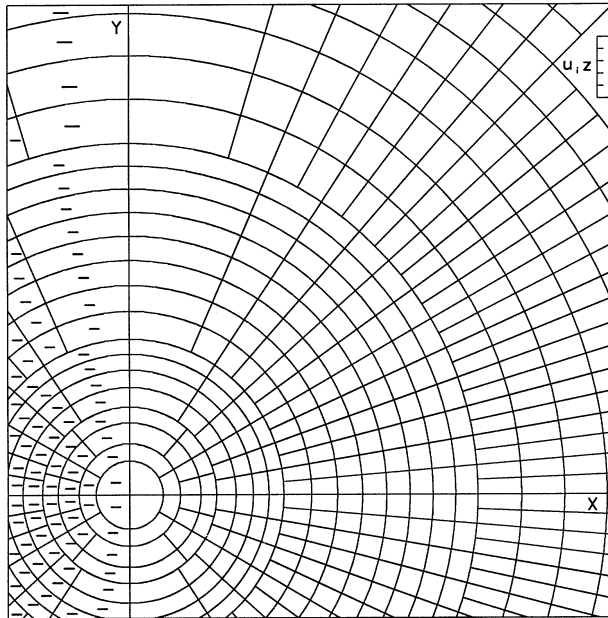


**Fig. 2.** Influence chart for  $aH_i$  (influence value per block is  $\pm 0.004$ , negative influences are indicated by a minus, (-), sign)

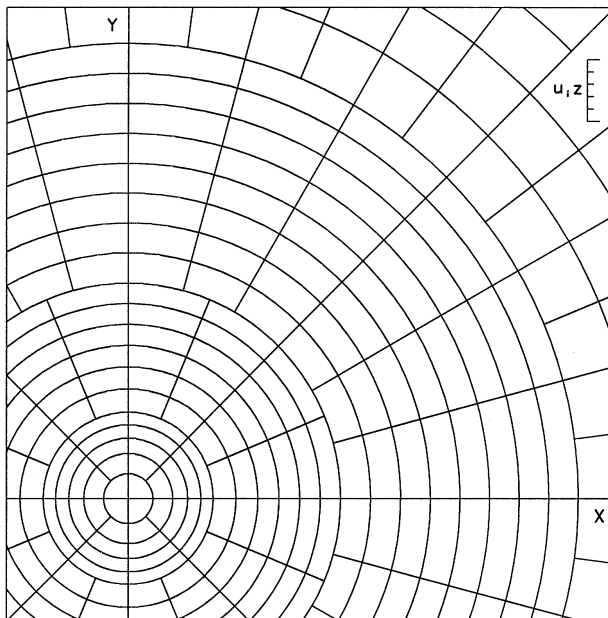


**Fig. 3.** Influence chart for  $cF_i$  (influence value per block is 0.01)

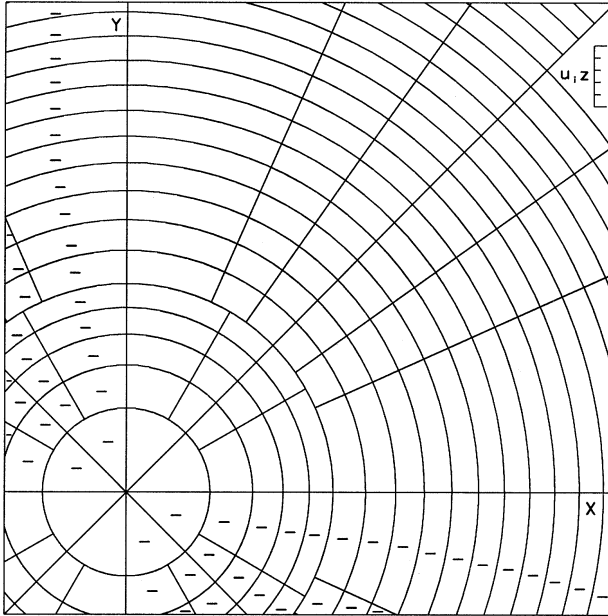


**Fig. 4.** Influence chart for  $dG_i$  (influence value per block is  $\pm 0.004$ , negative influences are indicated by a minus, (-), sign)

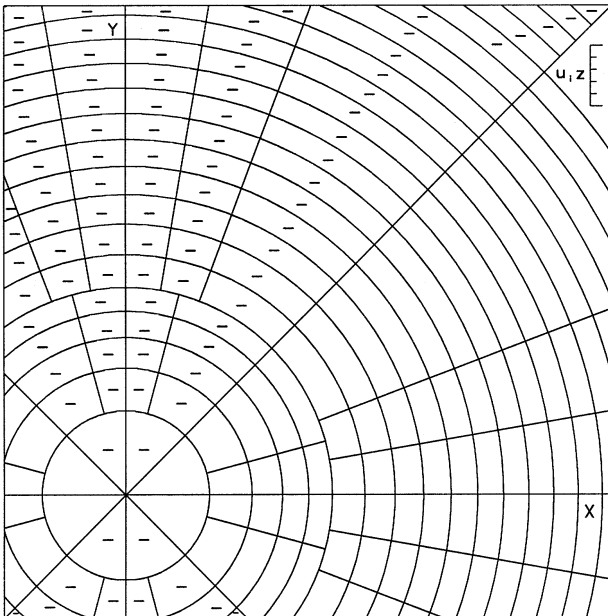


**Fig. 5.** Influence chart for  $eG_i$  (influence value per block is  $\pm 0.004$ , negative influences are indicated by a minus, (-), sign)



calculating the vertical displacement in a half-space subjected to a uniform normal load for case 3 material.

### 3.3 Closed-Form Solutions and the Influence Charts for Surface Displacements

Equations (3)–(5) are limited to solving the displacements in the interior of a transversely isotropic half-space subjected to three-dimensional uniform loads. Also, the proposed charts (Figs. 2–5) are only suitable for computing the displacements in the half-space subjected to irregularly-shaped surface loads. Practically, displacements at the surface of a half-space induced by surface loads are important. In order to prepare the influence charts for computing the surface displacements of a transversely isotropic half-space, the closed-form solutions for the surface displacements (at point O) have to be derived. The exact solutions for surface displacements can be derived from Eqs. (3)–(5) by setting  $z = 0$ . Then, the closed-form solutions for the surface displacements at point O due to uniform loads can be expressed as:

$$u_x^0 = \frac{\bar{P}_x}{2} L \left[ - \left( k - \frac{km}{u_1} - \frac{1}{u_3 C_{44}} \right) * c\mathbf{I} + \frac{1}{2\pi} \left( k - \frac{km}{u_1} + \frac{1}{u_3 C_{44}} \right) * e\mathbf{I} \right] \\ + \frac{\bar{P}_y}{4\pi} L \left( k - \frac{km}{u_1} + \frac{1}{u_3 C_{44}} \right) * d\mathbf{I} + \frac{\bar{P}_z}{2\pi} L k (u_2 - m) * a\mathbf{I}; \quad (8)$$

$$u_y^0 = \frac{\bar{P}_x}{4\pi} L \left( k - \frac{km}{u_1} + \frac{1}{u_3 C_{44}} \right) * d\mathbf{I} \\ + \frac{\bar{P}_y}{2} L \left[ - \left( k - \frac{km}{u_1} - \frac{1}{u_3 C_{44}} \right) * c\mathbf{I} - \frac{1}{2\pi} \left( k - \frac{km}{u_1} + \frac{1}{u_3 C_{44}} \right) * e\mathbf{I} \right] \\ + \frac{\bar{P}_z}{2\pi} L k (u_2 - m) * b\mathbf{I}; \quad (9)$$

$$u_z^0 = \frac{\bar{P}_x}{2\pi} L k (m - u_2) * a\mathbf{I} + \frac{\bar{P}_y}{2\pi} L k (m - u_2) * b\mathbf{I} + \bar{P}_z L k u_2 (m - u_1) * c\mathbf{I}, \quad (10)$$

where  $\mathbf{I} = r/L$ , and  $L$  is the base length for the surface displacements. The loaded area can be drawn to any scale whatever and the base length  $L$  determined for the particular scale used. Equations (8)–(10) indicate that the displacements can be computed from knowing the loads, the base length, the material constants, and the geometry of sector ( $a, b, c, d, e, \mathbf{I}$ ). Hence, one can draw the charts for  $a\mathbf{I}$ ,  $b\mathbf{I}$ ,  $c\mathbf{I}$ ,  $d\mathbf{I}$  and  $e\mathbf{I}$  for computing the three surface displacements, using graphical methods. Similarly to preparing the charts for interior displacements, except that the radii of the circles relate to the base length ( $L$ ) of surface displacements, the charts for  $a\mathbf{I}$ ,  $b\mathbf{I}$ ,  $c\mathbf{I}$ ,  $d\mathbf{I}$ , and  $e\mathbf{I}$  can be constructed. The chart for  $b\mathbf{I}$  is the same as for  $a\mathbf{I}$  if the X- and Y-axes are exchanged. Consequently, only four independent charts,  $a\mathbf{I}$  (Fig. 6),  $c\mathbf{I}$  (Fig. 7),  $d\mathbf{I}$  (Fig. 8), and  $e\mathbf{I}$  (Fig. 9) are needed for computing the surface displacements. The influence value of each unit block on surface displacements is 0.04 of load intensity for  $a\mathbf{I}$ ,  $d\mathbf{I}$  and  $e\mathbf{I}$ , and of 0.01 of load intensity for  $c\mathbf{I}$ , respectively. Since the base length  $L$  in the right corner of Figs. 6–9 is always

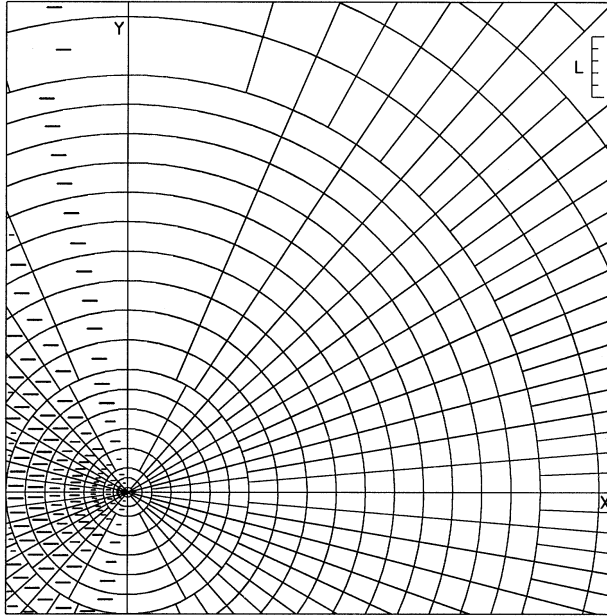


**Fig. 6.** Influence chart for  $aI$  (influence value per block is  $\pm 0.04$ , negative influences are indicated by a minus, (-), sign)

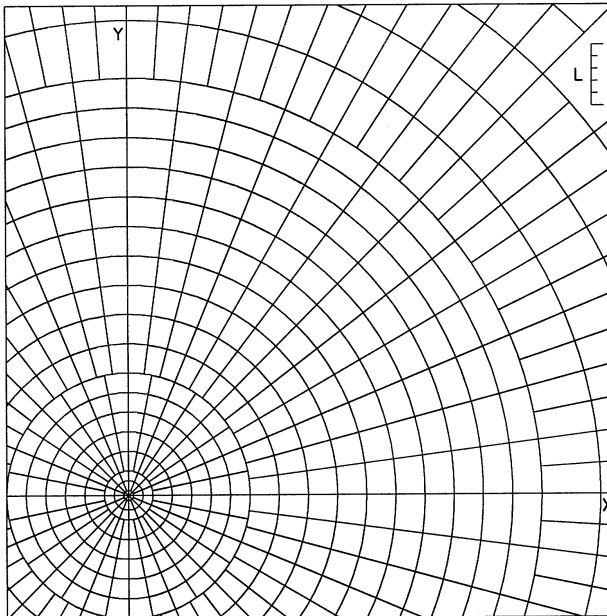


**Fig. 7.** Influence chart for  $cI$  (influence value per block is 0.01)

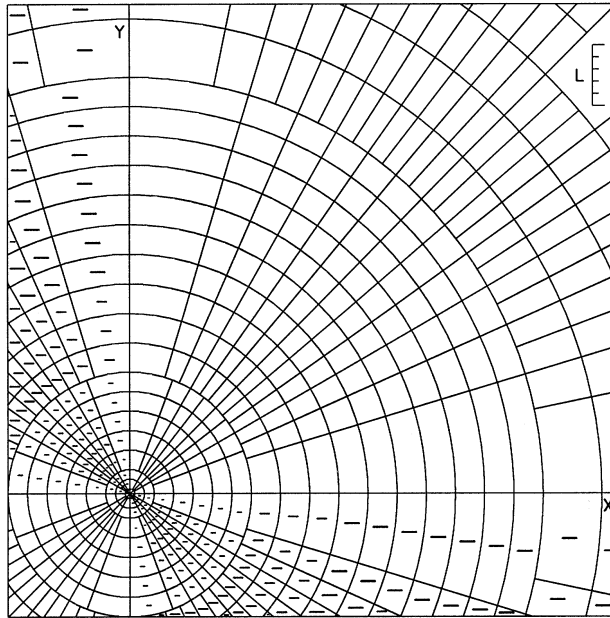


**Fig. 8.** Influence chart for  $dI$  (influence value per block is  $\pm 0.04$ , negative influences are indicated by a minus, (-), sign)

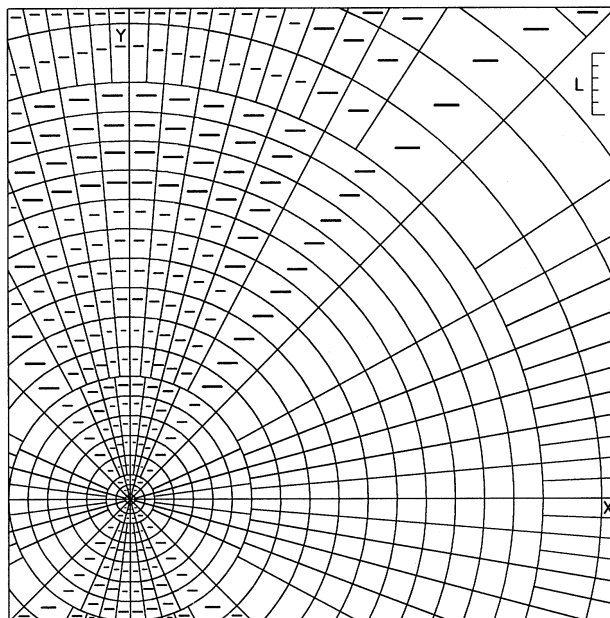


**Fig. 9.** Influence chart for  $eI$  (influence value per block is  $\pm 0.04$ , negative influences are indicated by a minus, (-), sign)

a real number (i.e., 0.8 cm), the values of  $L$  are unaffected by the media with conjugate complex roots (case 3) of the characteristic equation. Hence, the charts for  $aI$ ,  $cI$ ,  $dI$  and  $eI$  can be adopted to compute the surface displacements for all transversely isotropic rocks.

#### 4. Use of the Influence Charts

The three displacement components at a point in the interior or at the surface of the half-space subjected to three-dimensional loads on an arbitrary shape can be estimated from the new proposed influence charts. For this purpose, one must know (1) the elastic constants of half-space materials, (2) the types and magnitudes of surface loads, (3) the types of loading shapes, and (4) the depth of desired point ( $u_{iz}$ ) or the base length ( $L$ ) of the surface displacements. Detailed procedure to use the influence charts and their applications are described as follows:

- (1) Identify the type of rock (i.e., isotropic, transversely isotropic, orthotropic or generally anisotropic). If the rock is isotropic, the desired displacements can be computed using the Newmark charts (1947). However, the charts can only be used to compute the vertical displacement beneath/at the surface of an elastic mass induced by a uniform normal load. If the rock is orthotropic or generally anisotropic, there are no influence charts available.
- (2) Verify if the planes of isotropy are parallel to the surface. The influence charts presented herein are applicable only if the planes of isotropy are parallel to the surface.
- (3) Determine the root type of characteristic equation [i.e., case 1, 2 or 3, in Eq. (7)] for the half-space. Continue to step (4) through step (9) if the root type is case 1 or case 2. If the root type is case 3, the influence charts will have to be prepared individually and the following steps do not apply.
- (4) Calculate the characteristic root  $u_i$  ( $i = 1, 2, 3$ ), functions  $m$  and  $k$  from Eqs. (5) and (6).
- (5) Adopt a scale that should be equal to the depth  $u_{iz}$  ( $i = 1, 2, 3$ ) as shown in Figs. 2–5 for the interior displacements, or equal to the base length  $L$  in Figs. 6–9 for the surface displacements.
- (6) Redraw the plan of the loaded area, using the scale obtained in step (5). Transparent paper is recommended.
- (7) Place the plan of the loaded area plotted in step (6) on the influence charts. The point at which the displacements are desired should be placed over the center of the circles on these charts.
- (8) Count the number of blocks on the influence charts covered by the plan of the loaded area.
- (9) Compute the interior displacements from Eqs. (3)–(5), or the surface displacements from Eqs. (8)–(10), based on functions  $m$ ,  $k$  [from step (4)] and the number of blocks covered by plan of the loaded area [from step (8)].

Figure 10 presents a flow chart that illustrates the use of the influence charts. Although the charts are proposed for uniform loads, the displacement induced by

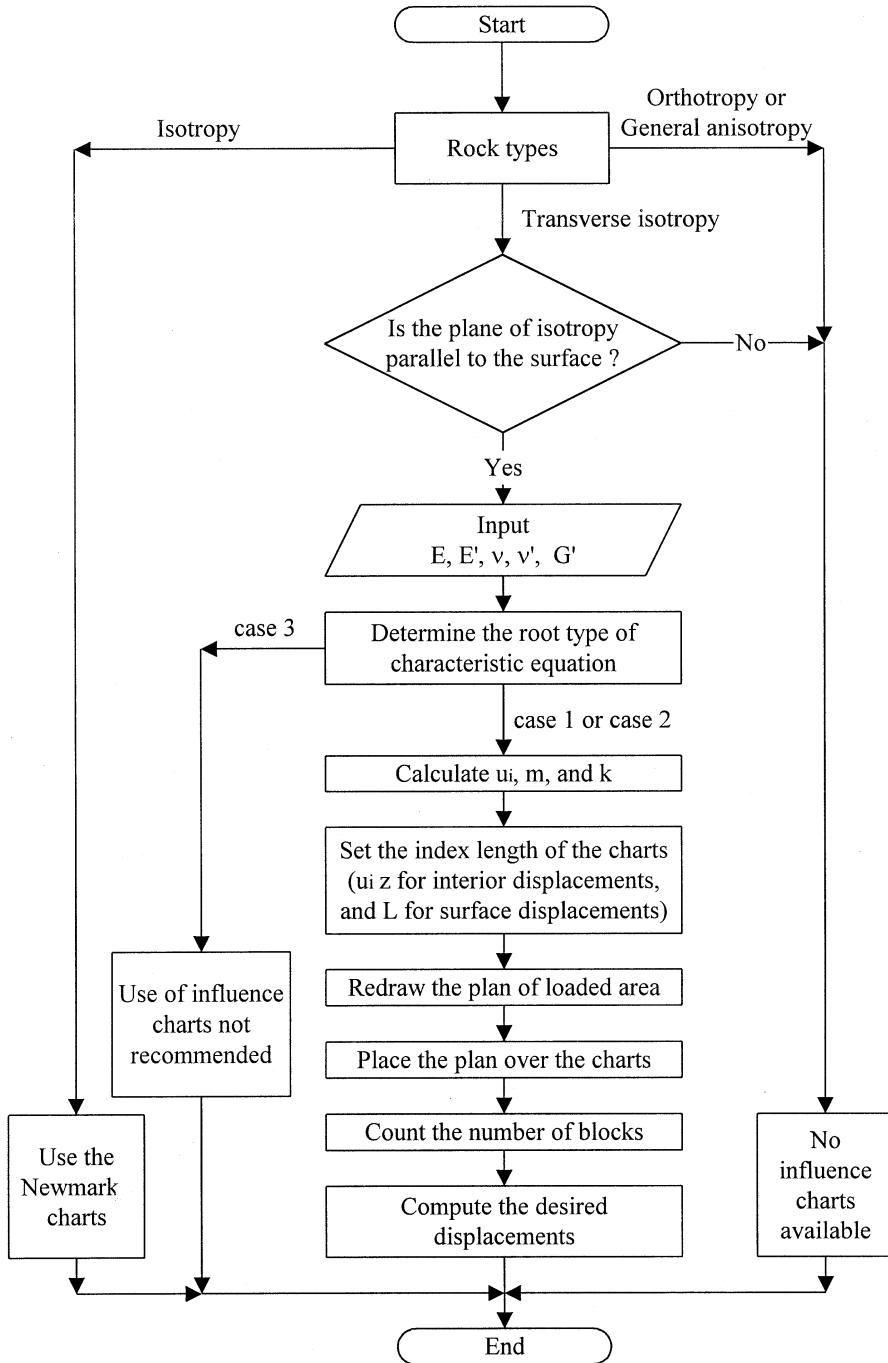


Fig. 10. Flow chart for computing the displacements induced by irregular loading shapes using influence charts

non-uniform loads can be estimated by dividing the entire loading area into several sub-areas, each with an approximately uniform load.

### 5. Illustrative Example

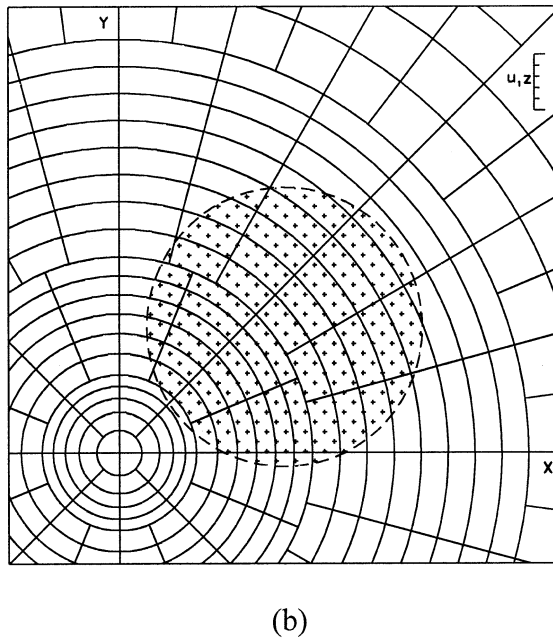
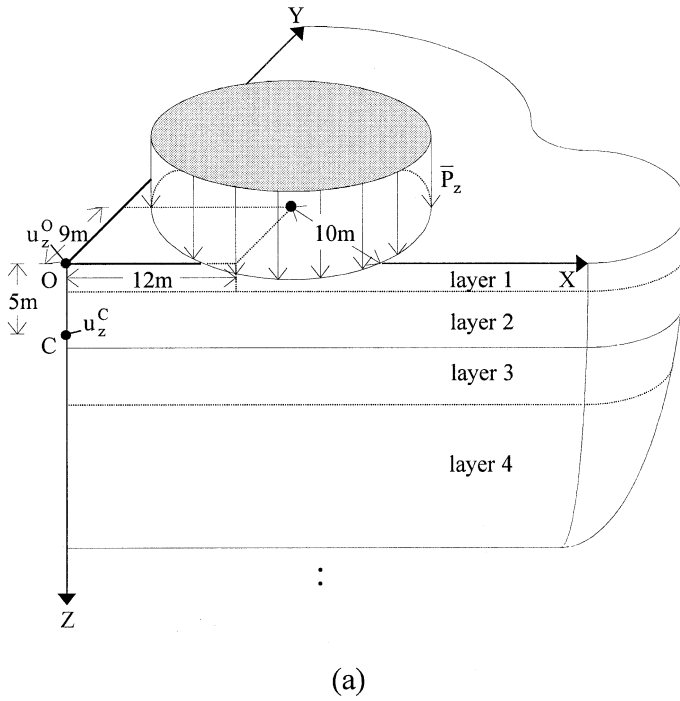
To demonstrate and verify the usage of the proposed displacement influence charts, an example is illustrated in this section. The interior and surface displacements of a half-space constituted by the layered rocks subjected to a uniform circular-shaped load are computed (Fig. 11a). The load with circular shape is chosen because there are several analytical solutions (i.e., Hanson and Puja, 1996) for verifying the results obtained from the presented graphical methods.

Fig. 11a shows that the vertical displacement at point C ( $u_z^C$ ) with a depth of 5 meters below the surface point O is desired. The layered rocks can equivalently be transversely isotropic rock, and the planes of transverse isotropy are parallel to the horizontal surface. The equivalent transversely isotropic properties of the layered rocks can be obtained from Wardle and Gerrard (1972). The mechanical properties of the hypothetical layered rock are given in Table 1. This ten-layer hypothetical rock satisfies the assumption of Salamon's model (1968) that the representative sample must contain a large number of layers. The deformability properties ( $E_i, \nu_i$ ) of the hypothetical layers are adopted from Kulkawy (1975) for various sedimentary rocks obtained from uniaxial compression tests. The adopted  $E_i$  increases with the increase of depth. Then, the five equivalent elastic constants of the layered rock are  $E = 42.5$  GPa,  $E' = 30.5$  GPa,  $\nu = 0.24$ ,  $\nu' = 0.14$ ,  $G' = 13.3$  GPa. The calculated five elastic constants satisfy the chosen domains of Gerrard (1975) and Amadei et al. (1987) for most transversely isotropic rocks. From Eq. (7), the medium belongs to case 1 with two real distinct roots. The half-space is subjected to a uniform normal load ( $\bar{P}_z$ ) on the horizontal surface with a loading area shown in Fig. 11a. Equation (5) then is rewritten as:

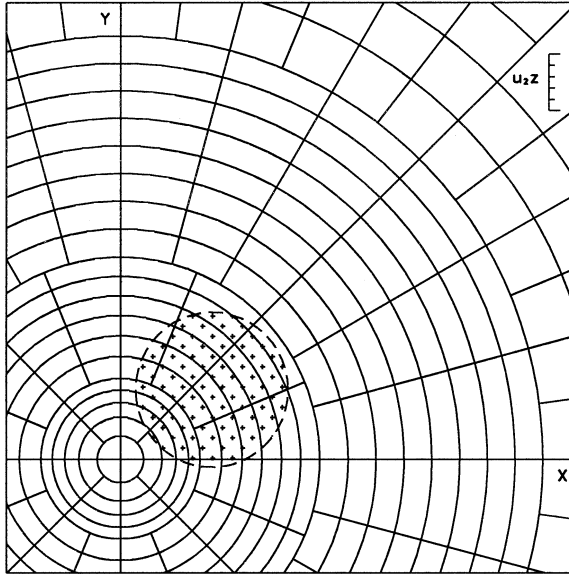
$$u_z^C / \bar{P}_z = 2ku_1u_2z * (m * cF_1 - u_2 * cF_2). \quad (11)$$

Equation (11) indicates that, knowing the elastic constants,  $u_i$ ,  $m$ , and  $k$ , one independent influence chart  $cF_i$  (Fig. 3) is enough for computing the normalized vertical displacement  $u_z^C / \bar{P}_z$  in this example. For illustration, the procedures of calculating  $u_z^C / \bar{P}_z$  are described as follows:

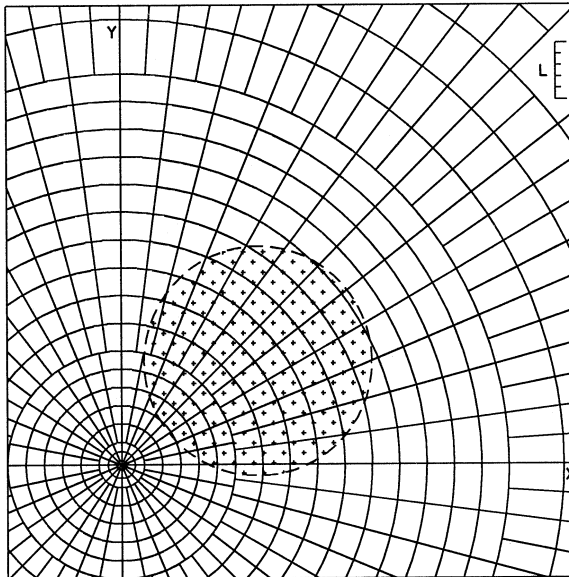
- (1) Calculate the characteristic roots and functions  $m$  and  $k$ :  $u_1 = 0.801$ ,  $u_2 = 1.495$ ,  $m = 2.224$  and  $k = 0.029$ .
- (2) Set the unit length as:  $u_1z = 4.005$ ,  $u_2z = 7.475$  for  $cF_1$  and  $cF_2$ , respectively.
- (3) Redraw the plan of the loaded area, using the scales obtained in step (2) on transparent papers (for  $cF_1$  and  $cF_2$ ).
- (4) Place the transparent papers prepared in step (3) on the influence chart ( $cF_i$ ). Point C should be placed over the center of the chart. Figs. 11b and 11c demonstrate the procedure for overlapping planes of the loaded area on the chart for  $cF_1$  and  $cF_2$ , respectively.
- (5) Count the numbers of blocks of blocks on Fig. 11b and Fig. 11c covered by



**Fig. 11a, b.** **a** Plan of loaded area acting on the surface, **b** the blocks covered by the plan of the loaded area for  $cF_1$



(c)



(d)

**Fig. 11c, d.** **c** The blocks covered by the plan of the loaded area for  $cF_2$ , **d** the blocks covered by the plan of the loaded area for  $cI$



**Table 1.** Thickness and deformability properties of sedimentary rocks for the illustrative layered rock

Rock layer i	Rock type	Thickness $t_i$ (m)	$E_i$ (GPa)	$\nu_i$
1	conglomerate	2.0	13.0	0.15
2	subgraywacke	4.0	14.6	0.07
3	sandstone	4.0	18.4	0.21
4	marlstone	10.0	19.3	0.04
5	graywacke	10.0	20.1	0.08
6	siltstone	10.0	24.0	0.18
7	shale	10.0	26.0	0.09
8	limestone	10.0	47.5	0.23
9	dolomite	20.0	59.0	0.30
10	anhydrite	20.0	75.8	0.27

the loaded area. The numbers of blocks are about 41 in Fig. 11b, and 20 in Fig. 11c.

- (6) From Eq. (11), the normalized vertical displacement ( $u_z^C/\bar{P}_z$ ) at point C is computed as:

$$\begin{aligned} u_z^C/\bar{P}_z &= 2 * 0.029 * 0.801 * 1.495 * 5 * (2.224 * 41 - 1.495 * 20) * 0.01 \\ &= 0.2128(\text{m/GPa}). \end{aligned}$$

Comparing the result with analytic solutions of Hanson and Puja (1996), the vertical displacement computed using the influence chart agrees with the analytic result within 2%.

Also, the vertical surface displacement at point O ( $u_z^0$ ) is computed. For a uniform normal load acting on the horizontal surface shown in Fig. 11a, Eq. (10) can be rewritten as:

$$u_z^0/\bar{P}_z = Lku_2(m - u_1) * cI. \quad (12)$$

Equation (12) indicates that the normalized vertical surface displacement  $u_z^0/\bar{P}_z$  can be calculated from a single influence chart  $cI$  (Fig. 7). Figure 11d demonstrates the procedure for overlapping plan of the loaded area on the chart for  $cI$ . The base length ( $L$ ) is set to be 5 meters. Then, approximately 71 blocks are located in the loaded area of Fig. 11d. Hence, the value of  $u_z^0/\bar{P}_z$  [Eq. (12)] is equal to 0.2190. Comparing with the analytical result (0.2174), the difference between them is less than 1%. Similarly, one can easily compute the horizontal displacements ( $u_x^C, u_x^0, u_y^C, u_y^0$ ) following the above procedures.

## 6. Conclusions

Based on the derived closed-form solutions for displacements under the vertex of a uniformly loaded sector in a transversely isotropic half-space, four independent influence charts are proposed for calculating the three displacement components at

any point in the interior of a half-space subjected to three-dimensional surface loads on an irregularly-shaped area. Then, by setting  $z = 0$  in the derived solutions, another four influence charts for computing the surface displacements are also proposed. The desired displacements are computed from the charts by counting the number of elements covered by a plan of the loaded area, drawn to a proper scale and laid upon the charts. The influence values from the four influence charts are then summed up. Since the influence charts for computing the interior displacements are prepared on the basis of the index length ( $u_i z$ ), the proposed charts for computing the interior displacements are only suitable for a transversely isotropic half-space with real roots of the characteristic equation. However, the charts for calculating the surface displacements can be adopted for all transversely isotropic media because of the base length ( $L$ ) always being a real number. The new influence charts are easy to use, and the computed results are reasonably accurate. These charts offer a practical alternative to the analytical and numerical solutions.

### Acknowledgments

The authors wish to thank the National Science Council of the R.O.C. for financially supporting this research under contract No. NSC 86-2621-E009-011.

### Appendix: Illustration for Constructing the Influence Chart for Case 3

To demonstrate the construction and usage of influence charts for case 3, an example for computing the vertical displacement ( $u_z^C$ ) subjected to a uniform normal load ( $\bar{P}_z$ ) is illustrated. From Eq. (6),  $u_1 = \gamma - i\delta$ ,  $u_2 = \gamma + i\delta$ . Then, the normalized vertical displacement ( $u_z^C/\bar{P}_z$ ) can be expressed in terms of the central angle  $\beta$  and a depth ratio  $r/z$  as follows:

$$\begin{aligned} u_z^C/\bar{P}_z &= 2km u_1 u_2 z * cF_1 - 2k u_1 u_2^2 z * cF_2 \\ &= z * cF', \end{aligned} \quad (13)$$

where  $c = \frac{\beta}{2\pi}$ ,  $F' = k u_2 \left[ -u_1(m - u_2) + m \sqrt{\left(\frac{r}{z}\right)^2 + u_1^2} - u_1 \sqrt{\left(\frac{r}{z}\right)^2 + u_2^2} \right]$ .

Similar to the method for drawing the charts for  $aH_i$ ,  $cF_i$ ,  $dG_i$ , and  $eG_i$ , the chart for  $cF'$  can also be constructed, except that the elastic constants of the medium are involved in this chart. Assuming that the elastic constants are  $E = 50$  GPa,  $E' = 25$  GPa ( $E/E' = 2$ ),  $G/G' = 1$ , and  $\nu = \nu' = 0.25$ , and solving Eq. (6), the characteristic roots are complex and the values of  $\gamma$  and  $\delta$  are 1.0082 and 0.5914, respectively. Figure 12 is the influence chart for  $cF'$ . For a uniform load as shown in Fig. 11a and using  $z$  as the scale (right corner of Fig. 12), one can redraw the plan of the loaded area. The number of blocks covered by the loaded area is approximately 37. Using Eq. (13), the normalized vertical displacement  $u_z^C/\bar{P}_z$  is equal to 0.185 ( $= 5 * 37 * 0.001$ , m/GPa). The value is very close to the exact solutions (0.188) of Hanson and Puja (1996).

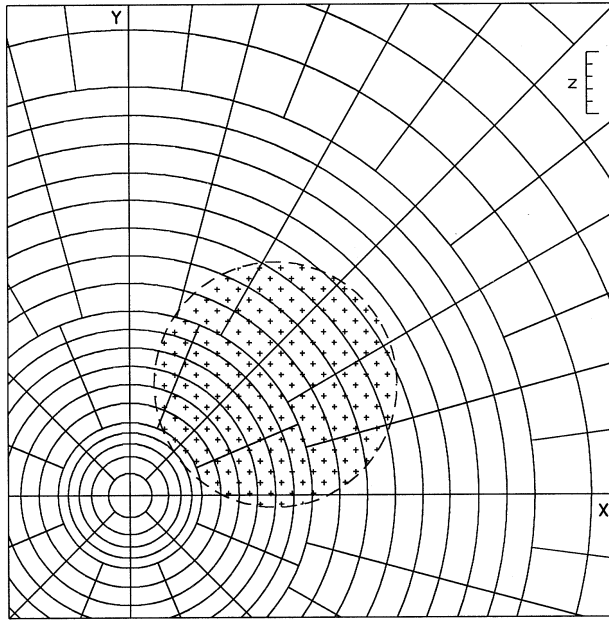


**Fig. 12.** Plan of loaded area on the influence chart for  $cF'$  ( $E = 50$  GPa,  $E' = 25$  GPa,  $G/G' = 1$ ,  $\nu = \nu' = 0.25$ , influence value per block is 0.001)

### List of Symbols

$a, b, c, d, e$	functions of central angle, $\beta$
$C_{ij}$ ( $i, j = 1 \sim 6$ )	elastic constants
$E, E', \nu, \nu', G'$	engineering elastic constants of a transversely isotropic rock
$E_i, \nu_i$	deformability properties of the $i$ -th layer of the layered rock
$F'$	functions of the complex roots $\gamma, \delta$ , and the depth ratio, $r/z$
$F_i, G_i, H_i$	functions of the depth ratio, $r/u_i z$ ( $i = 1, 2, 3$ )
$L$	the base length
$\bar{P}_j$ ( $j = x, y, z$ )	uniform loads (forces per unit of area)
$r$	radius of a circle
$r/u_i z$	the depth ratio
$t_i$	thickness of the $i$ -th layer of the layered rock
$u_1, u_2, u_3$	roots of the characteristic equation
$u_x^C, u_y^C, u_z^C$	interior displacements induced by irregularly-shaped loads
$u_x^0, u_y^0, u_z^0$	surface displacements induced by irregularly-shaped loads
$X, Y, Z$	Cartesian co-ordinate system
$\beta$	central angle
$\gamma, \delta$	real and imaginary part of the complex roots, respectively

### References

Amadei, B., Savage W. Z., Swolfs, H. S. (1987): Gravitational stresses in anisotropic rock masses. *Int. J. Rock Mech. Min. Sci. Geomech. Abstr.* 24, 5–14.

- Gerrard, C. M. (1975): Background to mathematical modeling in geomechanics: the roles of fabric and stress history. In: Proc., Int. Symp. on Numerical Methods, Karlsruhe, 33–120.
- Gradshteyn, I. S., Ryzhik, I. M. (1994): Tables of integrals. Series and products, Academic Press, San Diego, California.
- Hanson, M. T., Puja, I. W. (1996): Love's circular patch problem revisited: closed form solutions for transverse isotropy and shear loading. *Q. Appl. Math.* 54, 359–384.
- Huang, S. Y. (1995): Graphical solution for vertical stress distributions and settlement in soil due to uniformly applied vertical loads acting on a buried area. M.Sc. Thesis, The Cooper Union for the advancement of science and art.
- Kulhawy, F. H. (1975): Stress deformation properties of rock and rock discontinuities. *Engng. Geol.* 9, 327–350.
- Liao, J. J., Wang, C. D. (1998): Elastic solutions for a transversely isotropic half-space subjected to a point load. *Int. J. Numer. Anal. Methods Geomech.* 22, 425–447.
- Newmark, N. M. (1947): Influence charts for computation of vertical displacements in elastic foundations. Bull. No. 367, Eng. Expt. Station, University of Illinois.
- Poulos, H. G. (1967): The use of the sector method for calculating stresses and displacements in an elastic mass. In: Proc., 5th Aust.-New Zealand Conf. Soil Mech. Fndn. Engng., Auckland, 198–204.
- Salamon, M. D. G. (1968): Elastic moduli of a stratified rock mass. *Int. J. Rock Mech. Min. Sci.* 5, 519–527.
- Uzan, J., Ishai, I., Hoffman, M. S. (1980): Surface deflexion in a two-layer elastic medium underlain by a rough rigid base. *Geotechnique* 30, 39–47.
- Wang, C. D., Liao, J. J. (1998a): Elastic solutions for a transversely isotropic half-space subjected to buried asymmetric-loads. *Int. J. Numer. Anal. Methods Geomech* (in press).
- Wang, C. D., Liao, J. J. (1998b): Stress influence charts of transversely isotropic rocks. *Int. J. Rock Mech. Min Sci.* 35, 771–785.
- Wardle, L. J., Gerrard, C. M. (1972): The equivalent anisotropic properties of layered rock and soil masses. *Rock Mech.* 4, 155–175.

**Authors' address:** Prof. J. J. Liao, Department of Civil Engineering, National Chiao-Tung University, Hsinchu 30050, Taiwan, Republic of China.